Supplementary Information for

Enhancement of electrocatalytic abilities for reducing carbon dioxide: Functionalization with a redox-active ligand-coordinated metal complex

Habib Md Ahsan, Brian K. Breedlove,* Santivongskul Piangrawee, Mohammad Rasel Mian, Ahmed Fetoh, Goulven Cosquer, and Masahiro Yamashita

E-mail: breedlove@m.tohoku.ac.jp

Table of Contents

Experimental details

Characterization and Instrumentation. Single-crystal X-ray diffraction data were collected on a Bruker APEX-II diffractometer with an APEX II CCD detector and *JAPAN thermal Engineering Co., Ltd* Cryo system DX-CS190LD. The crystal structure was solved by using direct methods (SIR2004[1] or SHELXS-97[2]), followed by Fourier syntheses. Structure refinement was performed by using full matrix least-squares procedures using SHELXL-97[2] on F^2 in the Yadokari-XG 2009 software.[3] Elemental analysis and ESI-MS measurements were performed at the Research and Analytical centre for Giant Molecules, Tohoku University.

Electrochemistry. Electrochemistry was performed using an ALS/HCH Model 620D electrochemical analyser. A glassy carbon (3 mm diameter) electrode was used as a working electrode, Pt wire was used as a counter electrode, and Ag wire was used as a reference electrode. The supporting electrolyte was 0.1 M tetrabutylammonium hexafluorophosphate ($TBAPF_6$) in dry CH_3CN and in 5% H_2O and CH_3CN (v/) solution mixture. N_2 and CO_2 gas were bubbled into the solutions at least 30 min before cyclic voltammetry was performed. All potentials were converted to NHE.

Controlled Potential Electrolysis. Controlled potential electrolysis (CPE) experiments were performed by using an ALS/HCH Model 620D electrochemical analyser. A Gamry five-neck cell was used for all experiments. A cell was equipped with three Ace-Thread ports used for each electrode and two joints used for gas purging and gas collection after electrolysis. A piece of Pt wire was used for the counter electrode and Ag wire for reference electrode. Both are separated from the bulk solution by the porous frit. A glassy carbon working electrode was used for the working electrode (surface area 0.196 cm^2). The experiment was performed using 0.1 M $TBAPF_6$ in dry CH_3CN and 5% H_2O and CH_3CN (v/v) solution mixture. The solution was purged with CO_2 gas for 30 min before electrolysis. Gas-phase products were sampled using a gas-tight syringe to confirm CO_2 reduction product. A gas chromatograph (Agilent 6890N, 5975C) equipped with Agilent HP-MOLESIEVE, length 30 m, ID, 0.32 mm, film 12 µm columns was used for product identification. Helium (99.99%) was used as the carrier gas, *m/z* range: 10–100. Gas chromatography calibration curve was prepared using a known volume of CO gas. CPE measurements were performed at three times for every sample. The faradic efficiency was calculated by dividing the actual amount of CO produce during control potential experiment (CPE), and the amount of CO expected based on the charge passed during the CPE experiments. The Turnover frequency (TOF) was calculated based on Eq. 1. The reported TOF and faradic efficiency are averaged values.

Syntheses of 1, 2 and 3

All chemicals were reagent grade obtained from commercial sources and used without further purification. Quinolone-2-carbaldehyde (pyridine-2-carbonyl) hydrazone (qlca) was synthesized following a reported procedure.[4] *cis*-$[Ru(bpy)_2Cl_2]$ was prepared according to the reported procedure.[5]

Synthesis of $[Ru(bpy)_2(qlca)]$ (1). To a solution of the qlca (276 mg, 1 mmol) in ethanol (50 mL) in a round bottle flask was added 484 mg (1 mmol) of *cis*-$[Ru(bpy)_2Cl_2]$. The solution mixture was reflux for 8 h. The solvent was removed under reduced pressure. The solid was purified by chromatography over Bio-beads S-X1 with CH_2Cl_2. The first fraction was collected, and the solvent evaporated to obtain black-red solid (yield 80%). ESI-MS: *m/z* = 669.13. Anal. Calcd for $C_{36}H_{28}N_8ORuCl$: C, 59.62; H, 3.89; N, 15.45%. Found: C, 59.71; H, 3.81; N, 15.47%.

Synthesis of $[Ru(bpy)_2(NiCl_2qlca)]Cl$ (2). 1 (69 mg, 0.1 mmol) was dissolved in 10 mL of ethanol, and then nickel chloride·$6H_2O$ (23 mg, 0.1 mmol) was added. The mixture was stirred at room temperature for 6 h, during which a blackish red precipitate formed. The precipitate was collect and washed with ethanol. Black plate-type single crystals were obtained 3–4 days later from methanol/diethyl ether (yield: 75%). ESI-MS: *m/z* = 817.00. Anal. Calcd for $C_{36}H_{27}N_8Cl_3ONiRu$: C, 50.64; H, 3.19; N, 13.12%. Found: C, 50.59; H, 3.27; N, 13.15%.

Synthesis of $[qlcaNiCl_2]$ (3). qlca (376 mg, 1 mmol) was dissolved in 15 mL of ethanol, and one drop of triethylamine was added. Nickel chloride·$6H_2O$ (23 mg, 1 mmol) was dissolved in 10 mL ethanol, and the solution was added to the solution containing the ligand. The mixture was stirred for 1 h at room temperature, during which a precipitate formed. The precipitate was collected and washed with ethanol (yield: 92%). ESI-MS: *m/z* (M^-) = 402.97.

Electrospray ionization mass spectrometry (ESI-MS) of 1

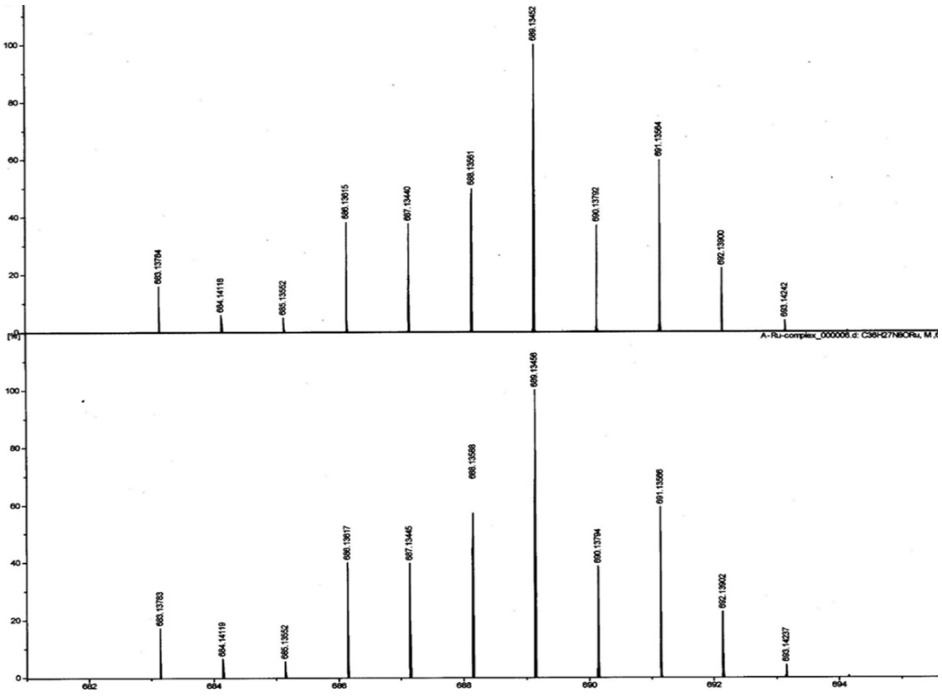

Fig. S1: ESI mass spectrum of **1** with simulation (upper) and experimental (lower)

Electrospray ionization mass spectrometry (ESI-MS) of 2

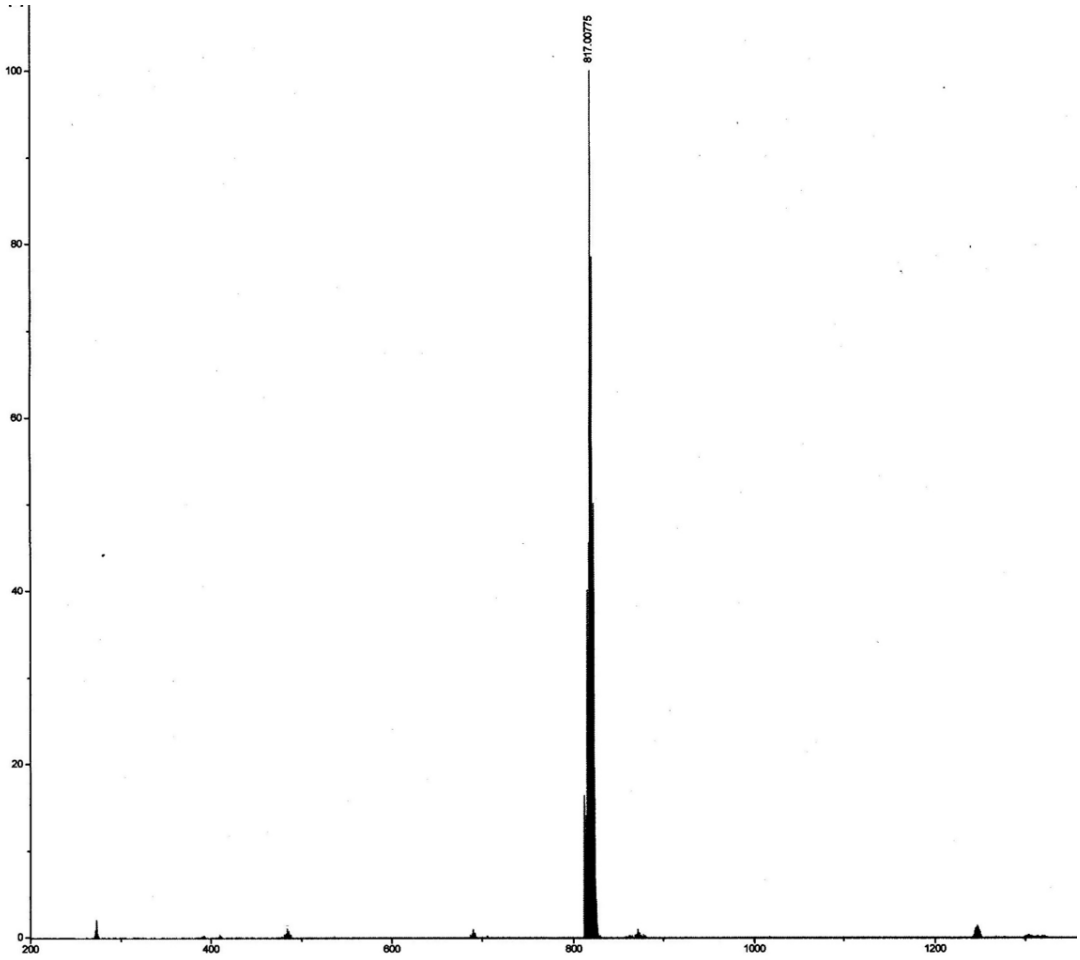

Fig. S2: ESI mass spectrum of **2**

Crystallographic parameters for 2

Table S1. Crystallographic details for **2**.

Radiation type, wavelength (Å)	Mo Kα, 0.71073
Formula*	$C_{37}H_{38}Cl_3N_8NiO_5Ru$
Formula weight (g/mol)	948.64
Crystal system	monoclinic
Space group	$P2_1$
Crystal size (mm^3)	$0.3 \times 0.2 \times 0.06$
a (Å)	12.458(7)
b (Å)	11.207(7)
c (Å)	15.772(9)
β (deg)	101.850(8)
V ($Å^3$)	2155(2)
Z	2
Temperature (K)	93
Calcd density (g/cm^3)	1.462
μ (mm^{-1})	1.023
R_1, wR_2 [$I > 2\sigma(I)$]	0.0507, 0.1139
R_1, wR_2 [all data]	0.0623, 0.1207
R_{int}	0.0385
F(000)	967
GOF	1.075
Flack parameter	0.17(6)

*Formula do not include 0.43 H_2O solvent molecule

Cyclic voltammograms of 3 with addition of $[Ru(bpy)_2]^{2+}$

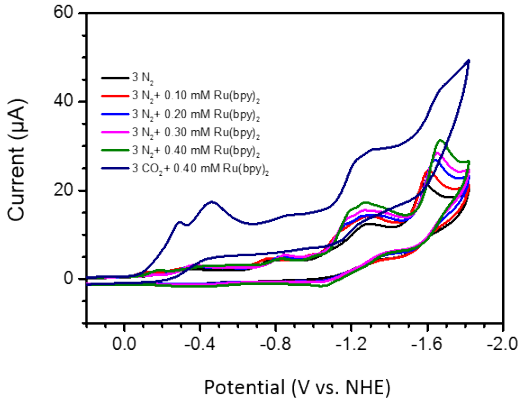

Fig. S3. Cyclic voltammgrams of (0.5 Mm) **3** in 5% H_2O and CH_3CN solution mixture with $TBAPF_6$ with adding different amount of $[Ru(bpy)_2]$. Scan rate 0.1 V/s.

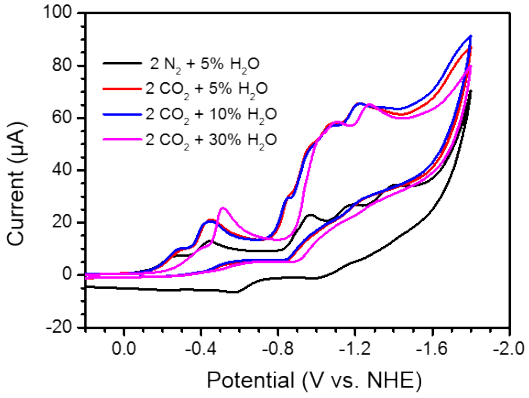

Fig. S4. Cyclic voltammgrams of **2** (0.5 mM) in H_2O/CH_3CN mixtures with different amounts of H_2O containing $TBAPF_6$. Scan rate 0.1 V/s.

Cyclic voltammograms of 2 with addition of water

Diffusion coefficient D calculation from cyclic voltammograms for 2

The randles-Sevcik equation

$$i_p = 0.4463 n_p FA[cat](n_p FvD/RT)^{1/2}$$

where i_p is the peak current (A), n_p is the number of electron(s) involved in the redox system (1 for Ni(II/I) redox process), F is the Faraday constant (96500 $C mol^{-1}$), A is the surface area of working electrode (0.071 cm^2), [cat] is catalysts concentration (mol/cm^3) , v is the scan rate (V/s), R is the universal gas constant (8.31 $JK^{-1}mol^{-1}$), and T is the temperature (298 K). An i_p vs $v^{1/2}$ plot was made from cyclic voltammograms data at different scan rates (Fig. S6) to determine D (4.86×10^{-5} cm^2s^{-1}).

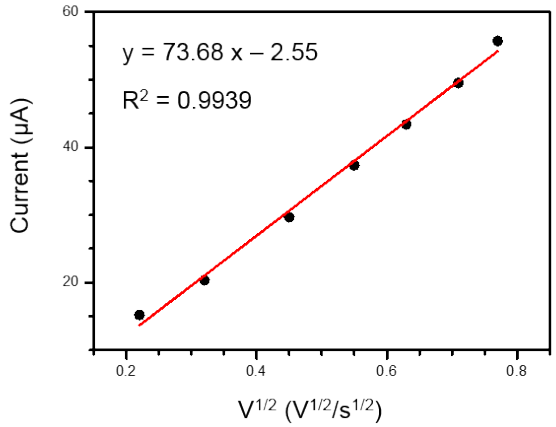

Fig. S6. i_p vs. $v^{1/2}$ plot for **3**, data collected from Fig. S5.

Diffusion coefficient D calculation from cyclic voltammograms for 3

The randles-Sevcik equation

$$i_p = 0.4463 n_p FA[cat](n_p FvD/RT)^{1/2}$$

Where, i_p is peak current (A), n_p is the number of electron(s) involves in redox system (1 for Ni(II/I) redox process), F is the Faraday constant (96500 $Cmol^{-1}$), A is the surface area of working electrode (0.071 cm^2), [cat] is catalysts concentration (mol/cm^3) , v is the scan rate (V/s), R is the universal gas constant (8.31 $JK^{-1}mol^{-1}$), and T is the temperature (298 K). An i_p vs $v^{1/2}$ plot was made from cyclic voltammograms data at different scan rates (Fig. S8) to determine D (5.13×10^{-5} cm^2s^{-1}).

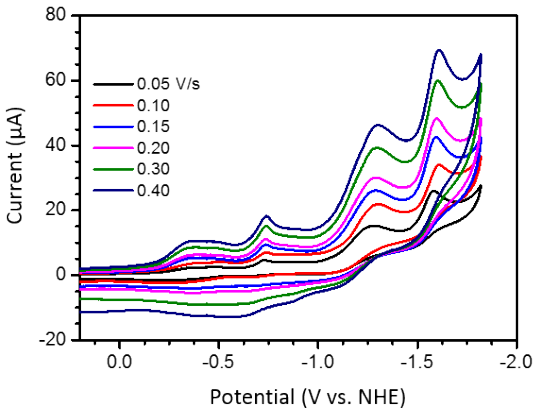

Fig. S7. Cyclic voltammgrams of **3** (0.5 mM) in 5% H_2O/CH_3CN solution mixture with $TBAPF_6$ at different scan rates. The Ni(II/I) couples are consider for cathodic peak current.

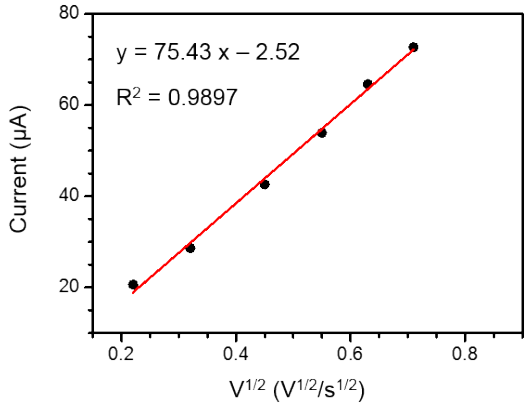

Fig. S8. i_p vs. $v^{1/2}$ plot for **3**, data collected from Fig. S7

TOF calculation based on CPE data for 2 and 3

The calculation of TOF for based CPE for CO generation followed by Eq. 1, which is modified by McCrory et al.,[6] from saveant and co-workers.[7,8]

$$TOF = \frac{(i_{el})^2\,(1 + exp\left[\frac{F}{RT}\left(E_{app} - E_{\frac{1}{2}}\right)\right])}{F^2 A^2 D[cat]^2} \qquad Eq.\,1$$

Here, i_{el} is average current of CPE for CO generation (*A*), *F* is faraday constant (96500 $Cmol^{-1}$), *R* is the universal gas constant (8.31 $JK^{-1}mol^{-1}$), *T* is the temperature (298 *K*), E_{app} is the applied potential during CPE, *A* is the surface area of working electrode (0.196 cm^2) , *D* is the diffusion coefficient for catalyst and [*cat*] is the concentration of catalyst in solution. $E_{1/2}$ is the redox potential of Ni(II/I) couple (–1.20 V) for **2** and the redox potential for Ni(II/I) couple (–1.30 V) for **3**, All data summarized in Table S2.

Table S2. Control potential electrolysis data for **2** and **3**

Catalysts	Conditions	Potential (V vs. NHE)	Charge/C	TOF s^{-1}	FE % for CO	Overpotential (mV)
Blank	5% H_2O and CH_3CN (v/v)	–1.55	0.01			
2	Dry CH_3CN	–1.40	0.42	1.31	31	680
2	5% H_2O and CH_3CN (v/v)	–1.20	1.10	120	82	480
3	5% H_2O and CH_3CN (v/v)	–1.55	0.18	0.83	60	830

All CPE were performed 30 minute. Catalysts concentration 0.5mM. TOF calculated from Eq. 1 and current consider based on FE value.

References

1 M. C. Burla, R. Caliandro, M. Camalli, B. Carrozzini, G. L. Cascarano, L. D. Caro, C. Giacovazzo, G. Polidoria and R. Spagnac, *J. Appl. Cryst.,* 2005, **38**, 381–388.

2 G. M. Sheldrick, *Acta Crystallogr.,* 2008, **A64**, 112–122.

3 Wakita, K. Yadokari-XG, Software for Crystal Structure Analyses; 2001; Release of Software (Yadokari-XG 2009) for Crystal Structure Analyses, C. Kabuto, S. Akine, T. Nemoto and E. Kwon, *J. Crystallogr. Soc. Jpn.,* 2009, 51, 218–224.

4 A. Mori, T. Suzuki, Y. Sunatsuki, M. Kojima and K. Nakajima, *Bull. Soc. Jpn.,* 2015, **88**, 186–197.

5 G. A. Lawrance, D. R. Stranks and S. Suvachittanont, *Inorg. Chem.,* 1978, **17**, 3322–3325.

6 W. Nie, C. C. L. McCrory, *Chem. Commun*., 2018, **54**,1579–1582.

7 C. Costentin, S. Drouet, M. Robert and J. M. Saveant, *Science,* 2012, **338**, 90–94.

8 C. Costentin, M. Robert and J. M. Saveant, *Chem. Soc. Rev.,* 2013, **42**, 2423–2436.